# The two human centrin homologues have similar but distinct functions at *Tetrahymena* basal bodies

Tyson Vonderfecht, Michael W. Cookson, Thomas H. Giddings, Jr., Christina Clarissa, and Mark Winey
Department of Molecular, Cellular, and Developmental Biology, University of Colorado–Boulder, Boulder, CO 80309

**ABSTRACT** **Centrins are a ubiquitous family of small $Ca^{2+}$-binding proteins found at basal bodies that are placed into two groups based on sequence similarity to the human centrins 2 and 3. Analyses of basal body composition in different species suggest that they contain a centrin isoform from each group. We used the ciliate protist *Tetrahymena thermophila* to gain a better understanding of the functions of the two centrin groups and to determine their potential redundancy. We have previously shown that the *Tetrahymena* centrin 1 (Cen1), a human centrin 2 homologue, is required for proper basal body function. In this paper, we show that the *Tetrahymena* centrin 2 (Cen2), a human centrin 3 homologue, has functions similar to Cen1 in basal body orientation, maintenance, and separation. The two are, however, not redundant. A further examination of human centrin 3 homologues shows that they function in a manner distinct from human centrin 2 homologues. Our data suggest that basal bodies require a centrin from both groups in order to function correctly.**

**Monitoring Editor**
Fred Chang
Columbia University

Received: Jun 13, 2012
Revised: Oct 11, 2012
Accepted: Oct 12, 2012

## INTRODUCTION

The basal body is an important microtubule organizing center (MTOC) widely found in eukaryotes, except for yeast and higher plants, and is responsible for nucleating and organizing the ciliary axoneme and anchoring it at the surface of the cell. Cilia are microtubule-based appendages that play key roles in cell locomotion, fluid flow, and mechanosensory, chemical sensory, or photosensory functions (Marshall and Nonaka, 2006). Aberrations in ciliary or basal body function have been associated with several human diseases, such as Meckel-Gruber syndrome and polycystic kidney disease (Badano *et al.*, 2006). The importance of basal bodies is further highlighted by their ability to be interconverted with centrioles, components of the centrosome, which is involved in mitotic spindle formation (Bornens and Azimzadeh, 2007).

The basal body has a key role in the regulation of ciliary function. For example, basal bodies in the multiciliated cells of the oviduct epithelium are specifically orientated to produce directional fluid flow that transports the egg from the ovaries to the uterus (Marshall and Kintner, 2008). Likewise, the maintenance of the basal body is important, and an incorrectly maintained basal body will likely disrupt ciliary functions. We have previously identified centrin as a protein involved in both basal body orientation and maintenance (Stemm-Wolf *et al.*, 2005; Vonderfecht *et al.*, 2011). Centrins are a ubiquitous family of small $Ca^{2+}$-binding proteins found at MTOCs (Salisbury *et al.*, 1984; Huang *et al.*, 1988; Andersen *et al.*, 2003; Keller *et al.*, 2005; Kilburn *et al.*, 2007; Liu *et al.*, 2007; Hodges *et al.*, 2010; Carvalho-Santos *et al.*, 2011). Structurally, they consist of two domains connected by a short linker, with each domain containing a pair of EF hands, a $Ca^{2+}$-binding motif (Veeraraghavan *et al.*, 2002; Hu and Chazin, 2003; Matei *et al.*, 2003; Yang *et al.*, 2005; Li *et al.*, 2006; Thompson *et al.*, 2006). Alignments of centrins

This article was published online ahead of print in MBoC in Press (http://www.molbiolcell.org/cgi/doi/10.1091/mbc.E12-06-0454) on October 19, 2012.

Address correspondence to: Mark Winey (mark.winey@colorado.edu).

Abbreviations used: BSA, bovine serum albumin; Cen1, *Tetrahymena* centrin 1; Cen2, *Tetrahymena* centrin 2; *cen2Δ*, *cen2* null; CTD, C-terminal domain; FITC, fluorescein isothiocyanate; GFP, green fluorescent protein; immuno-EM, immuno–electron microscopy; KD, kinetodesmal; MTOC, microtubule organizing center; MTT, metallothionein; NTD, N-terminal domain; PBS, phosphate-buffered saline; RT-PCR, reverse transcriptase PCR; SPP, super-peptose; TBS, Tris-buffered saline.

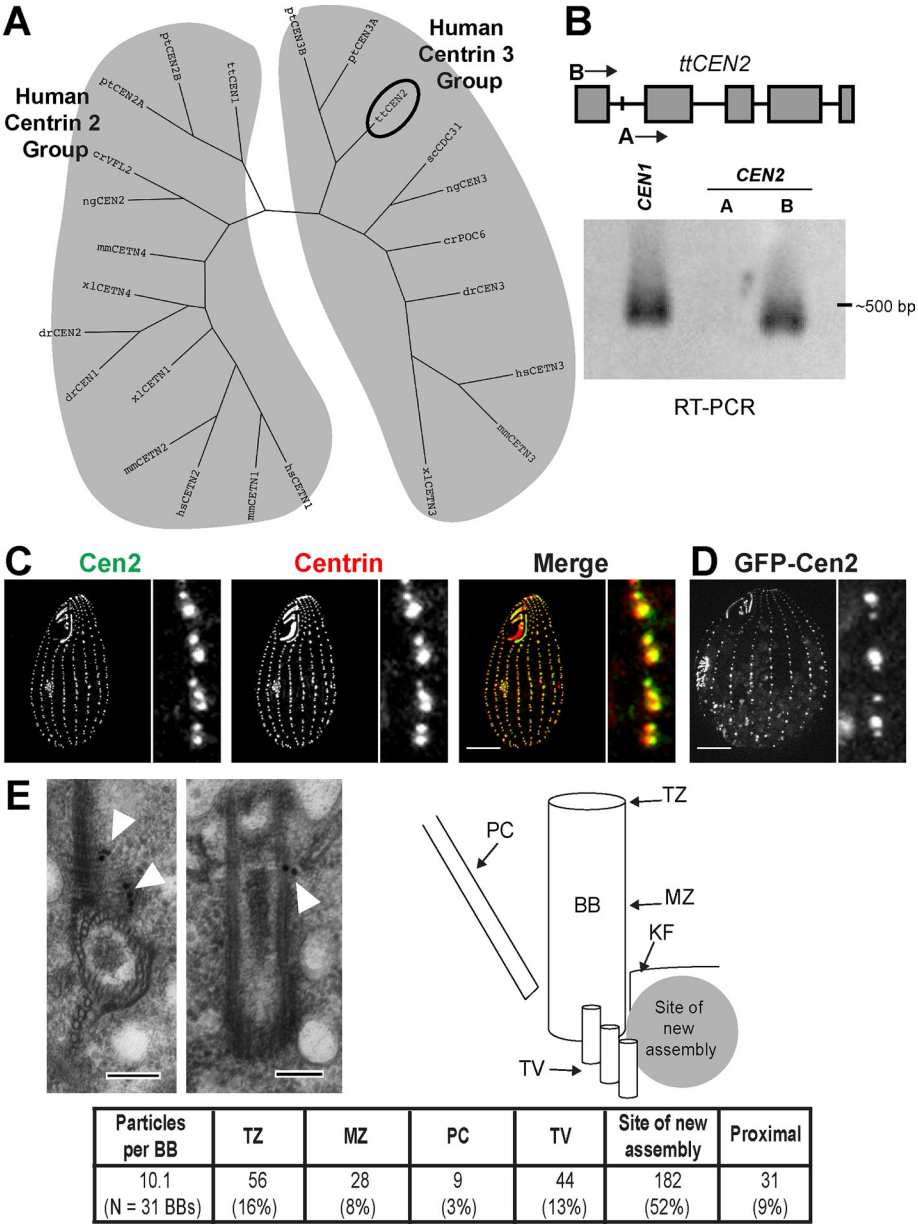


| Particles per BB | TZ | MZ | PC | TV | Site of new assembly | Proximal |
|---|---|---|---|---|---|---|
| 10.1 (N = 31 BBs) | 56 (16%) | 28 (8%) | 9 (3%) | 44 (13%) | 182 (52%) | 31 (9%) |

FIGURE 1: Basal bodies have two centrin isoforms and the *Tetrahymena* Cen2 localizes to basal bodies. (A) A phylogenetic tree showing the two centrin groups as defined by homology to the human centrins 2 and 3. The circle indicates the location of the *Tetrahymena CEN2*. cr, *Chlamydomonas reinhardtii*; dr, *Danio rerio*; hs, *Homo sapiens*; mm, *Mus musculus*; ng, *Naegleria gruberi*; pt, *Paramecium tetraurelia*; sc; *Saccharomyces cerevisiae*; tt, *Tetrahymena thermophila*; xl, *Xenopus laevis*. (B) Top, the *CEN2* locus. Gray boxes are the exons. "A" and "B" are the locations of the primers used for RT-PCR. Bottom, RT-PCR showing that *CEN2* is expressed. *CEN1* was used as a positive control. (C) Cen2 localizes to basal bodies. Green, anti-Cen2; red, centrin (20H5 antibody). Scale bar: 10 µm. (D) Localization of GFP-Cen2. Scale bar: 10 µm. (E) Immuno-EM showing localization of GFP-Cen2. Left, cross-section; Right, longitudinal view. The table shows the particle distribution to various regions of the basal body. BB, basal body; KF, KD fiber; MZ, mid-zone; PC, postciliary microtubules; TV, transverse microtubules; TZ, transition zone. Scale bar: 100 nm.

from a wide range of organisms show that centrins separate into two groups (Figure 1A). These two groups are annotated based on sequence similarity to the human centrins, centrin 2 and centrin 3 (Middendorp *et al.*, 1997; Laoukili *et al.*, 2000; Bornens and Azimzadeh, 2007). Despite this separation, the two groups share high sequence similarity (74.4% for the human centrins 2 and 3). Analyses of centriole or basal body composition in different species suggests that they contain a centrin isoform from each group (Figure 1A; Andersen *et al.*, 2003; Keller *et al.*, 2005; Kilburn *et al.*, 2007; Liu *et al.*, 2007). Most vertebrates have two centrins belonging to the human centrin 2 group, with one that appears to be ubiquitously expressed and the other expressed only in ciliated cells (Wolfrum and Salisbury, 1998; Laoukili *et al.*, 2000). Budding yeast has only one centrin isoform (Cdc31p, a human centrin 3 homologue); however, the spindle pole body, the only MTOC in yeast, has no structural similarity to a basal body or centriole (Jaspersen and Winey, 2004), suggesting that having the two centrin isoforms at basal bodies or centrioles has been conserved throughout evolution (Bornens and Azimzadeh, 2007).

To date, studies on centrin function at basal bodies and centrioles have largely focused on those belonging to the human centrin 2 group. Members of this group localize to the distal end of the basal body or centriole and sites of new assembly (Sanders and Salisbury, 1994; Paoletti *et al.*, 1996; Geimer and Melkonian, 2005; Stemm-Wolf *et al.*, 2005; Kilburn *et al.*, 2007). Human centrin 3 is also found at these sites (Laoukili *et al.*, 2000), suggesting that the two groups share similar localization. Analyses on the function of human centrin 2 and its homologues suggest that this group is involved in basal body or centriole maintenance, assembly, orientation of assembly, and separation of the daughter from its mother (Spang *et al.*, 1993; Salisbury *et al.*, 2002; Koblenz *et al.*, 2003; Ruiz *et al.*, 2005; Stemm-Wolf *et al.*, 2005; Yang *et al.*, 2010; Vonderfecht *et al.*, 2011). Human centrin 3 may play a role in centrosome duplication (Middendorp *et al.*, 2000), but the nature of its function remains unclear. Studies in *Paramecium* (Ruiz *et al.*, 2005; Aubusson-Fleury *et al.*, 2012) and *Trypanosoma brucei* (Selvapandiyan *et al.*, 2012) have shown that knockdown of centrin isoforms yields differing effects on basal bodies, suggesting that the two centrin groups may have nonredundant functions; however, this hypothesis has not been fully tested. Cdc31p, the only yeast centrin, is the most-studied human centrin 3 homologue. It has been shown to be required for the duplication of the spindle pole body (Hartwell *et al.*, 1973; Byers, 1981; Baum *et al.*, 1986); however, since the yeast MTOC is structurally different from a basal body or centriole (Jaspersen and Winey, 2004), it remains to be seen whether the function of Cdc31p is conserved throughout the human centrin 3 group.

The role of centrins at vertebrate centrioles has been extensively studied, and the data suggest that centrins may play a role in

regulating the rate of centriole assembly but are not required for completing centriole assembly (Kleylein-Sohn *et al.*, 2007; Strnad *et al.*, 2007; Yang *et al.*, 2010; Dantas *et al.*, 2011; Lukasiewicz *et al.*, 2011). Studies examining the role of centrins at vertebrate basal bodies are sparse; however, it has been shown that the human centrins are up-regulated during ciliogenesis in epithelial tissue cultures (LeDizet *et al.*, 1998). Furthermore, an RNA interference screen identified human centrin 2 as important for ciliogenesis (Graser *et al.*, 2007). Morpholinos that target the human centrin 2 homologue in zebra fish lead to defects commonly associated with ciliopathies (Delaval *et al.*, 2011). This accumulating body of evidence suggests that centrins function primarily at the basal body. The small number of studies on the human centrin 3 group at basal bodies and the fact that the two centrins share high sequence similarity raise two major questions: what is the function of this group and are the two centrin groups redundant, meaning do basal bodies need both centrin isoforms? To answer these two questions, we used the ciliate protist *Tetrahymena thermophila* as a model system for basal body biology. Basal bodies in *Tetrahymena* are found within cortical rows, which are rows of basal bodies that run along the posterior to anterior axis of the cell, and within the oral apparatus, a feeding structure at the anterior end of the cell (Frankel, 2000; Pearson and Winey, 2009). We have previously identified four centrins in *Tetrahymena*, with centrin 1 (Cen1) and centrin 2 (Cen2) localizing only to basal bodies (Stemm-Wolf *et al.*, 2005). Like the human centrins, Cen1 and Cen2 share high sequence similarity (78.4%). We have shown that Cen1 is essential and is involved in basal body stability, assembly, orientation of assembly, and separation (Stemm-Wolf *et al.*, 2005; Vonderfecht *et al.*, 2011). We were unable to detect the expression of Cen2 (Stemm-Wolf *et al.*, 2005); however, our *Tetrahymena* basal body proteome shows that Cen2 exists at basal bodies (Kilburn *et al.*, 2007), and a *Tetrahymena* microarray study identified expression of the Cen2 gene, *CEN2* (Miao *et al.*, 2009).

We wished to gain a better understanding of the functions of the two centrin groups by determining Cen2's role at basal bodies and whether Cen1 and Cen2 are redundant. We found that while Cen1 and Cen2 share similar functions, they are distinct from each other, suggesting that basal bodies require a centrin from each group to function correctly.

## RESULTS

### Cen2 is expressed and localizes to basal bodies

A *Tetrahymena* microarray study identified the expression of *CEN2* (Miao *et al.*, 2009), and our basal body proteome identified Cen2 as a component (Kilburn *et al.*, 2007). However, we have been unable to detect expression of *CEN2* by Northern blotting (Stemm-Wolf *et al.*, 2005). At the start of this study, the *Tetrahymena* genome underwent an extensive reannotation, and the newly annotated *CEN2* showed that the previously predicted start codon was an intron. We performed reverse transcriptase PCR (RT-PCR) and were able to detect product only by using a primer that anneals to the newly annotated start codon (Figure 1B), confirming that *CEN2* is expressed. The cDNA product was sequenced, and translation shows that it encodes a centrin protein. The only differences between the correct sequence and the misidentified sequence lie in the first 20 residues, which make up the N-terminal tail of the protein (Supplemental Figure S1). The new protein sequence of Cen2 indicates that it is still a human centrin 3 homologue (Figures 1A and S1).

We generated a polyclonal peptide antibody that specifically recognizes the N-terminal extension of Cen2 (Figures S1, S2A, and S2B). With the αCen2 antibody, we were able to detect Cen2 at all basal bodies in the cortical rows and oral apparatus (Figure 1C), confirming that Cen2 is a basal body component. Immuno–electron microscopy (immuno-EM) was performed to determine Cen2's localization within the basal body. The αCen2 antibody predominantly labeled regions at the site of new assembly at the proximal end of the basal body (Figure S2C). This was surprising because centrins generally localize to both the site of new assembly and the distal end of the basal body (Sanders and Salisbury, 1994; Laoukili *et al.*, 2000; Geimer and Melkonian, 2005; Stemm-Wolf *et al.*, 2005; Kilburn *et al.*, 2007). We reasoned that the αCen2 antibody is not sensitive enough to label the distal end and generated a cell line expressing Cen2 tagged with green fluorescent protein (GFP), which localizes to basal bodies (Figure 1D). We observed labeling by a αGFP antibody at the distal end of the basal body, at or near the transition zone, with most of the labeling concentrated at the site of new assembly (Figure 1E). This localization slightly differs from Cen1, which also localizes to the midzone of the basal body (Stemm-Wolf *et al.*, 2005; Kilburn *et al.*, 2007). In all, our results show that Cen2 is expressed in *Tetrahymena* and localizes to the site of new assembly and the distal end of the basal body. Our results also indicate that *Tetrahymena* basal bodies have a centrin isoform from the two centrin groups, a characteristic that appears to be conserved at basal bodies throughout evolution.

### Cen2 is required for basal body maintenance and orientation

Because the function of the human centrin 3 group at basal bodies is not well known, we wished determine the role of Cen2 at *Tetrahymena* basal bodies. To answer this question, we created a *cen2* null allele (*cen2*Δ) strain (Figures S2A and S3A). Unlike the *cen1* null allele, which is lethal, *cen2*Δ cells are viable and are able to divide for many generations, indicating that *CEN2* is not essential. We found that the levels of Cen1 remained unchanged in the *cen2*Δ compared with wild-type cells (Figure S3B), suggesting that Cen1 is not compensating for the loss of Cen2 in the *cen2*Δ.

We examined *cen2*Δ cells by light microscopy and observed that they swim significantly slower than wild-type cells (Figure 2A), suggesting that the loss of Cen2 leads to a basal body or ciliary defect. This led us to perform immunofluorescence microscopy on cycling cells using αCen1 and anti-kinetodesmal (KD) fiber antibodies as basal body markers (Figure 2B). The KD fiber is a basal body accessory structure composed of striated rootlets that extend from the basal body, oriented toward the anterior of the cell (Allen, 1969). We observed that *cen2*Δ cycling cells have basal body defects (Figure 2B). The same basal body defects were observed using the Sas6a antibody, which labels basal bodies and has a background signal from the KD fibers (Figure S3C; Culver *et al.*, 2009). The *cen2*Δ cells had gaps between basal bodies in their cortical rows (Figure 2B, arrow), suggesting that deletion of *CEN2* leads to a loss of basal bodies. Quantification showed that there is almost a 27% reduction in the number of cortical row basal bodies per cell in the *cen2*Δ (461 ± 54) compared with wild-type cells (630 ± 86; $p < 0.01$, $n = 25$ cells). The loss of basal bodies is not likely due to the inability to assemble new basal bodies because of the existence of the oral primordium (Figure 2B, white boxes), which is indicative of new basal body assembly (Wolfe, 1970; Kaczanowski, 1978; Frankel, 2000).

Next we asked whether the loss of basal bodies is due to maintenance defects. Cells were arrested by starvation to inhibit new basal body assembly (Pearson *et al.*, 2009), and we examined their ability to maintain their existing basal bodies by quantifying the number of cortical row basal bodies per cell after 24 and 48 h of cell arrest (Figure 2, C and D). The *cen2*Δ showed a 31% reduction in the number of basal bodies per cell between the two time points,

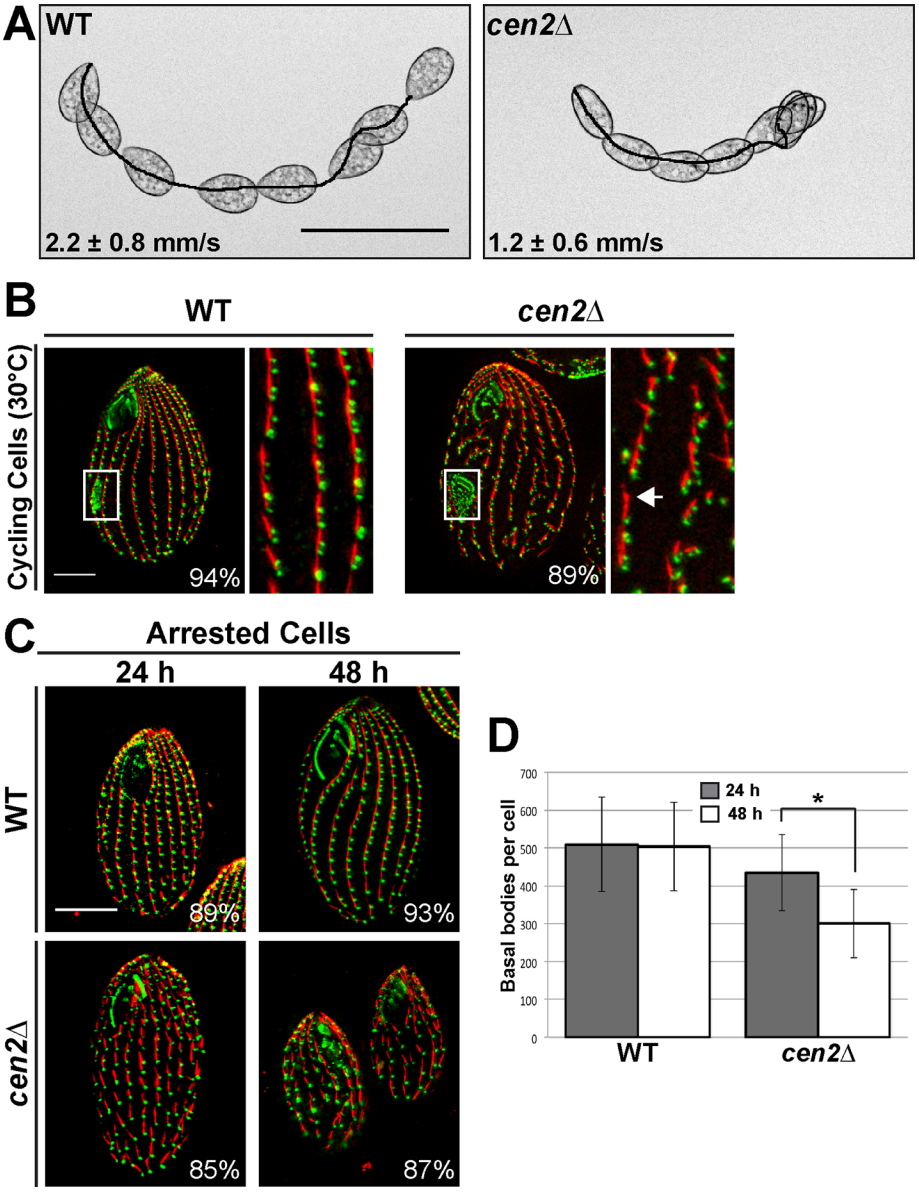


FIGURE 2: Deletion of *CEN2* leads to swimming defects and basal body maintenance defects. (A) Images showing the swimming speed of wild-type and *cen2*Δ cells. Scale bar: 100 μm. (B) Immunofluorescence images showing gaps (arrow) in the *cen2*Δ. White box, oral primordium, which is indicative of new basal body assembly. (C) Cells arrested by starvation and fixed 24 and 48 h after cell arrest. (B and C) Green, Cen1; red, KD fibers. Scale bar: 10 μm. Width of insets: 10 μm. Percentages indicate the frequency of observed phenotype for 100 cells. (D) Plot showing the number of basal bodies per cell at the two different time points. *, $p < 0.01$; $n = 25$ cells.

whereas wild-type cells displayed no significant reduction in the number of basal bodies per cell (Figure 2D; $p < 0.01$, $n = 25$ cells), showing that deletion of *CEN2* causes a loss of basal bodies due to maintenance defects.

We also observed basal bodies branching off within the cortical rows in the *cen2*Δ, suggesting that there is a basal body orientation defect. Basal body angle was measured to confirm the orientation defect (Figure 3A). We found that the *cen2*Δ had a large variation in basal body angle, with an average angle SD of 36 ± 3 degrees (Figure 3A). This was significantly different from wild type, which had an average angle SD of 7.8 ± 0.6 degrees (Figure 3A), confirming that Cen2 has a role in basal body orientation. EM analysis of the *cen2*Δ found examples of basal bodies branching off from cortical rows (Figure 3A). The KD fibers and postciliary microtubules of these basal bodies were not aligned with those of correctly positioned basal bodies. This suggests that the orientation defect in the *cen2*Δ might be a result of aberrantly rotated basal bodies. We also observed what appeared to be basal body separation defects in the *cen2*Δ. Cells were stained with αCen1, which labels all basal bodies (Stemm-Wolf *et al.*, 2005; Pearson *et al.*, 2009), and K-like antigen, which labels only mature basal bodies (Williams *et al.*, 1990; Shang *et al.*, 2002). Some mature basal body pairs in the *cen2*Δ were able to separate (Figure 3B, white arrows); however, some did not show proper separation (Figure 3B, blue arrows). This defect was observed on average a little more than three times per cell in the *cen2*Δ but less than one time per cell in wild-type cells ($n = 20$ cells). EM analysis of the *cen2*Δ showed two cilia sharing a single ciliary pocket (Figure 3C), which may be a result of the separation defect. In all, the analysis of the *cen2*Δ shows that deletion of *CEN2* leads to basal body maintenance, orientation, and separation defects.

To confirm that the observed basal body defects in the *cen2*Δ were due to deletion of *CEN2*, we introduced *CEN2* under control of the metallothionein (MTT) promoter into the *cen2*Δ genome by integration at the *RPL29* locus. The introduction of *MTT-CEN2* rescues the basal body maintenance and separation defects in the *cen2*Δ (Figures S3, D and E, and S4), confirming that Cen2 is required for basal body maintenance and orientation.

### Cen2 behaves differently from Cen1

The analysis of the *cen2*Δ strain suggests that Cen2 has a similar function to Cen1, leading to the question of whether the two proteins behave similarly at basal bodies. It was previously shown that all basal bodies, new and old, have the same levels of Cen1 (Figure 4A; Pearson *et al.*, 2009). With the αCen2 antibody, we observed that mature (old) basal bodies have brighter signals than immature (new) basal bodies (Figure 4A). The fluorescence of Cen1 or Cen2 labeling of new and old basal bodies was measured to calculate the new:old basal body fluorescence ratio (Figure 4A). The ratio was ~1 (0.96 ± 0.14) for Cen1, which is expected, since all basal bodies have equal amounts of Cen1 (Pearson *et al.*, 2009). As for Cen2, the ratio was 0.78 ± 0.28, and a Student's *t* test indicated that the two ratios are significantly different from each other ($p < 0.01$, $n = 50$ basal body pairs), showing that the old basal bodies have more Cen2 than the new basal bodies. To confirm this, we examined the labeling of Cen2 in arrested cells that were not undergoing new basal body assembly and whose basal bodies were all fully mature (Figure 4B; Pearson *et al.*, 2009). We observed equal labeling by the αCen2 antibody, with a fluorescence ratio

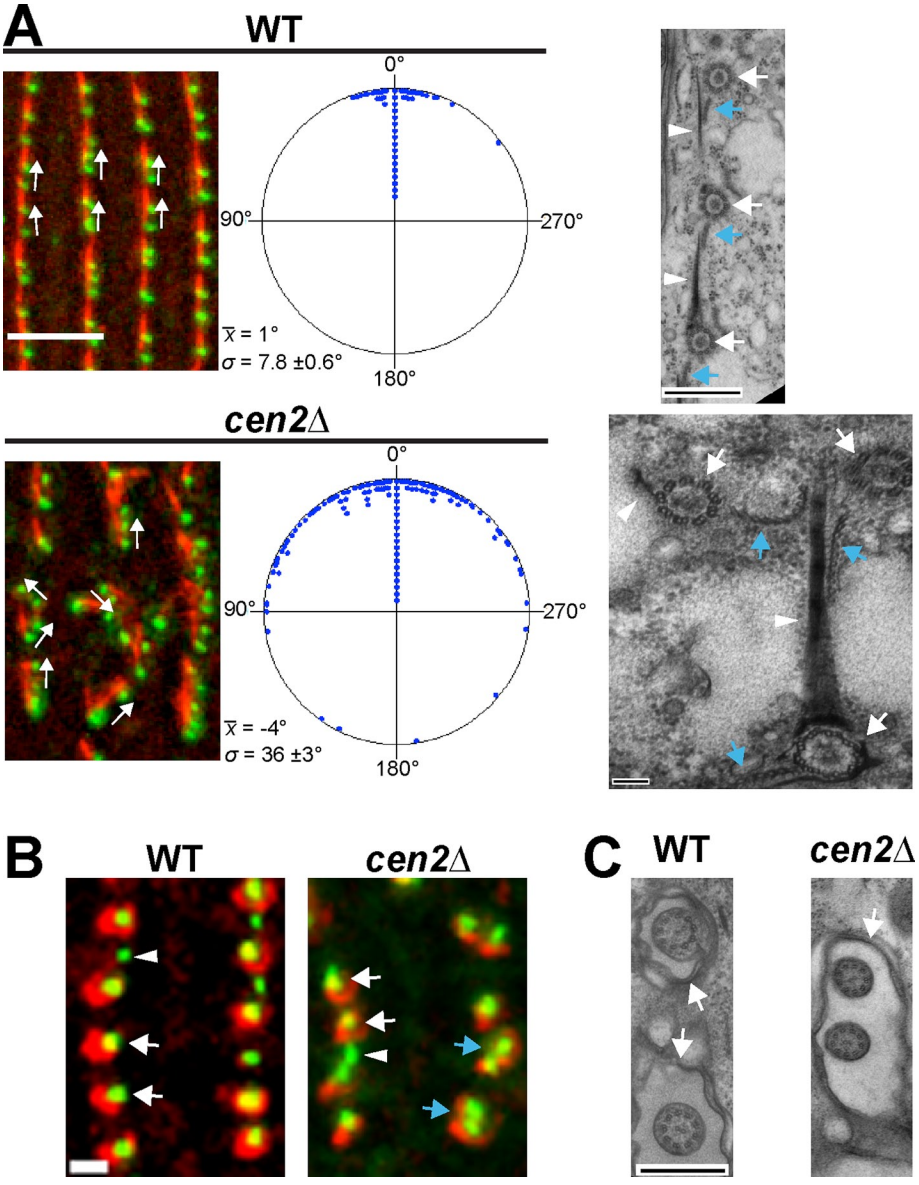


FIGURE 3: Deletion of *CEN2* leads to basal body orientation and separation defects. (A) Left panels show the basal body angle distribution for wild type and the *cen2*Δ. Green, Cen1; red, KD fibers. Scale bar: 5 μm. $\bar{x}$, average angle; σ, SD. In the circular plots, each point corresponds to five measurements in wild type and two measurements in the *cen2*Δ. $n = 200$ measurements. Right panels show electron micrographs of the basal body orientation defect. Basal bodies (white arrow) and their accessory structures (KD fiber, white arrowhead; postciliary microtubules, blue arrow) are rotated in *cen2*Δ cells. Scale bar: 500 or 100 nm (*cen2*Δ). (B) Close proximity of mature basal bodies suggests that there is a basal body separation defect in the *cen2*Δ (blue arrows). The average distance between a pair of old basal bodies is 1.5 ± 0.3 μm in wild type and 1.2 ± 0.4 μm in the *cen2*Δ, a significant difference ($n = 150$ basal body pairs). Green, Cen1; red, K-like antigen (mature basal body marker); white arrowhead, immature basal body; white arrow, mature basal body. Scale bar: 1 μm. (C) Electron micrographs showing that cilia in the *cen2*Δ share a ciliary pocket (arrow), whereas cilia in wild type do not. Scale bar: 500 nm.

near 1 (1.01 ± 0.21). The data show that Cen2 continues to accumulate at the basal body as it fully matures, suggesting Cen2 may have a role in basal body maturation. This is in contrast to Cen1, whose protein levels remain constant throughout the basal body's life cycle.

Next we wanted to determine whether the two domains of Cen2 behave in a manner similar to the domains of Cen1. We have previously shown that only the C-terminal domain (CTD) of Cen1 localizes to basal bodies (Vonderfecht *et al.*, 2011). Cen2's CTD and N-terminal domain (NTD) were tagged with GFP and expressed in a wild-type background containing endogenous wild-type Cen1 and Cen2. We found that, like Cen1, only the CTDs of Cen2 localize to basal bodies (Figure 4C). This suggests that the two centrin groups have similar modes of action, with the CTD involved in localization to basal bodies. In all, the data suggest that Cen1 and Cen2 have similar localization mechanisms but behave differently.

### The two centrin groups are distinct from each other

Because Cen1 and Cen2 have similar functions, we wanted to determine whether the two proteins have redundant functions at the basal body. If the two proteins are redundant, then overexpression of Cen1 in the *cen2*Δ should rescue the basal body phenotypes by compensating for the loss of Cen2. *CEN1* under control of the MTT promoter was introduced into *cen2*Δ, and it was observed that *CEN1* is overexpressed upon induction with $Cd^{2+}$ (Figure 5A). The *cen2*Δ *MTT-CEN1* cell line was examined by immunofluorescence, and we found that overexpression of *CEN1* is unable to compensate for the deletion of *CEN2*, as it was not capable of rescuing the loss of basal bodies and the orientation defects in the *cen2*Δ (Figures 5B and S4). The *CEN1* overexpression data suggest the two *Tetrahymena* basal body centrins are distinct.

Next we wanted to test whether that the two centrin groups are truly distinct by determining whether the human centrins can function similarly to their *Tetrahymena* centrin counterparts. To ensure that the human centrins 2 and 3 (*hsCETN2* and *hsCETN3*, respectively) localize to basal bodies, we tagged them with GFP and observed their localization to basal bodies in a wild-type background (Figure 5C). Next *hsCETN2* and *hsCETN3* under control of the MTT promoter were introduced into the *cen2*Δ. We found that only *hsCETN3* (the *Tetrahymena CEN2* homologue) rescues the loss of basal bodies and the orientation defects caused by the deletion of *CEN2*, whereas *hsCETN2* (the *Tetrahymena CEN1* homologue) could not (Figures 5D and S4). The *cen2*Δ *MTT-hsCETN3* cell line does not display complete rescue for some minor disorganization of the basal body cortical rows remains; however, the basal body orientation defect is not as severe as seen in *cen2*Δ (Figure S4). An examination of cells grown at elevated temperatures (38°C) showed that the increase in temperature exacerbated the loss of basal bodies and orientation defects in the *cen2*Δ whereas the *cen2*Δ *MTT-hsCETN3* cell line did not display any

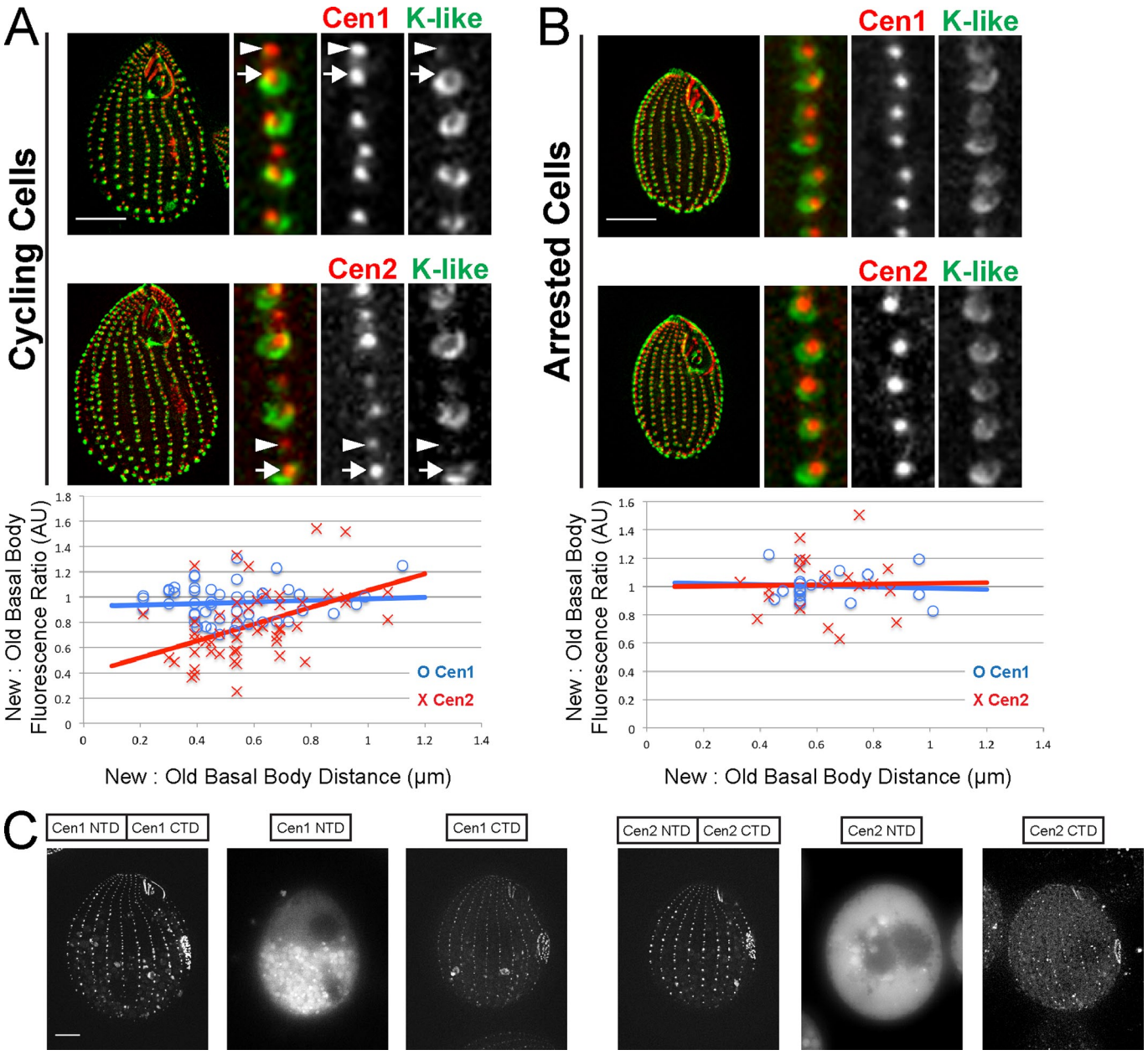


FIGURE 4: Cen2 behaves differently from Cen1. (A) Immunofluorescence images of cycling cells, showing that new (arrowhead) and old (arrow) basal bodies have equal levels of Cen1, while old basal bodies have higher levels of Cen2 than do new basal bodies. The plot shows the fluorescence ratio for the new and old basal body pairs vs. their distance. (B) Basal bodies in cells arrested by starvation have equal levels of Cen1 and Cen2, because all basal bodies are old (or mature). (A and B) Width of insets: 2.5 μm. Red, Cen1 (labels all basal bodies); green, K-like antigen (labels old basal bodies); AU, arbitrary units. (C) The CTD, but not the NTD, of Cen1 and Cen2 localize to basal bodies. Scale bars: 10 μm.

temperature-sensitive basal body phenotypes (Figures 5E and S4). In all, the data show that human centrin 3 functions similarly to *Tetrahymena* Cen2, confirming distinct functions for the two centrin groups.

### The domains between the two centrin groups are also distinct from one another

Because the two centrin groups have distinct functions at basal bodies despite a high degree of similarity, we wondered whether the NTD or the CTD was responsible for the separation of the two groups. An alignment the Cen1 and Cen2 domains showed that their CTDs were 91% similar, but their NTDs were 69% similar, suggesting that the NTD distinguishes between the two groups. To test this hypothesis, we introduced centrin chimeras composed of either Cen1's NTD with Cen2's CTD (the Cen1-Cen2 chimera) or Cen2's NTD with Cen1's CTD (the Cen2-Cen1 chimera) into the *cen2*Δ to determine which chimera would rescue the *cen2*Δ basal body phenotypes. Based on the alignments, it was expected that only the Cen2-Cen1 chimera would rescue the *cen2*Δ, since it contains Cen2's NTD. However, it was the Cen1-Cen2 chimera that unexpectedly rescued the loss of basal bodies and orientation defects in the *cen2*Δ at 30°C (Figures 6A and S4). For confirming that the Cen1-Cen2 chimera completely rescues the *cen2*Δ, cells were grown at 38°C to check for any temperature-sensitive basal body

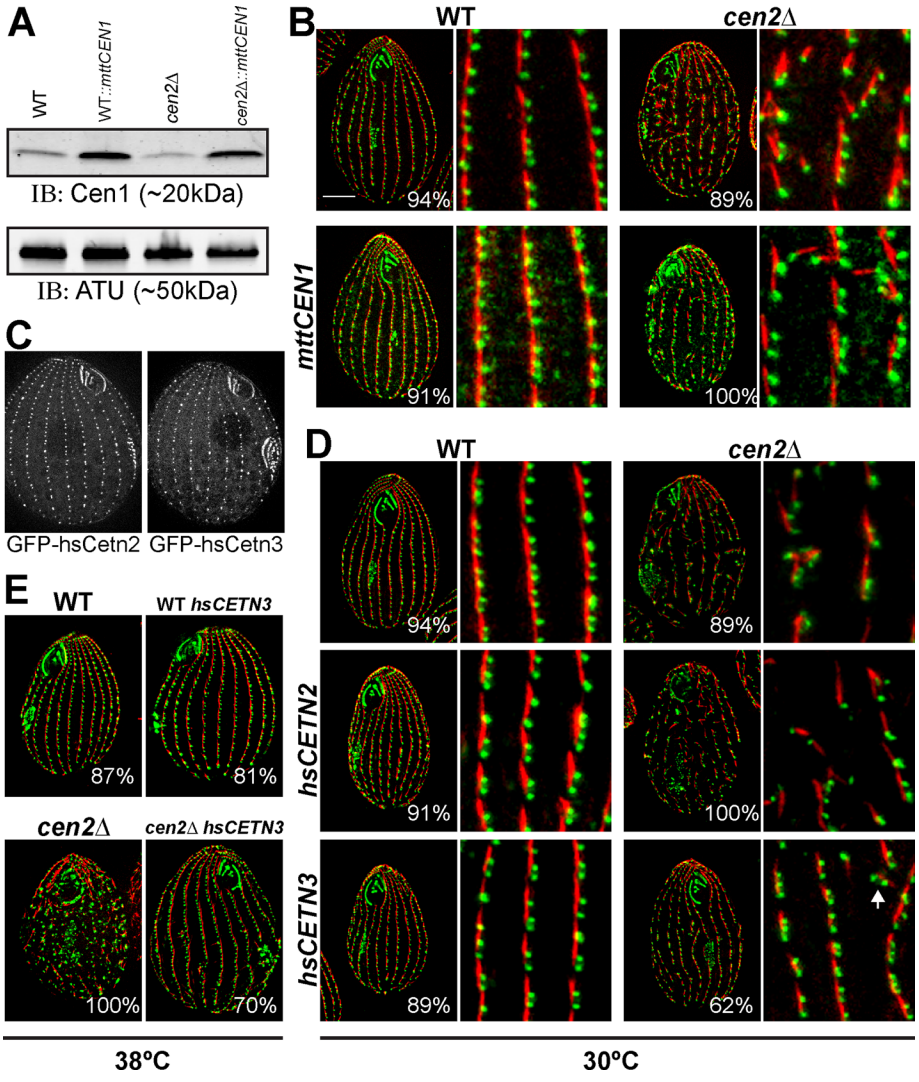


FIGURE 5: The two centrin groups are functionally distinct. (A) A Western blot showing Cen1 overexpression. α-Tubulin served as a loading control. (B) Immunofluorescence images showing that overexpression of *CEN1* is unable to rescue the *cen2*Δ. (C) Both GFP-hsCen2 and GFP-hsCen3 localize to basal bodies in *Tetrahymena*. (D and E) Immunofluorescence images showing that only *hsCEN3*, not *hsCEN2*, can rescue the *cen2*Δ basal body phenotypes at 30°C (D) and 38°C (E). Green, Cen1; red, KD fibers. Scale bar: 10 μm; width of insets: 10 μm; Percentages indicate the frequency of observed phenotype for 100 cells.

phenotypes. At this elevated temperature, we observed basal bodies branching from the cortical rows in the *cen2*Δ strain rescued by the Cen1-Cen2 chimera (Figure 6B, arrow). Quantification of the number of basal bodies per micrometer showed that there was no significant difference from wild type (Figure S4); however, there was more basal body angle variation in the *cen2*Δ strain rescued by the Cen1-Cen2 than in wild type (Figure S4). This indicates that the Cen1-Cen2 chimera in the *cen2*Δ is able to rescue the basal body loss defect but is unable to completely rescue the basal body orientation defect.

## DISCUSSION

Centriole and basal body structures consisting of triplet microtubules have two distinct centrins, one each similar to human *CENT2* and *CENT3* (Andersen *et al.*, 2003; Carvalho-Santos *et al.*, 2011; Hodges *et al.*, 2010; Keller *et al.*, 2005; Kilburn *et al.*, 2007; Liu *et al.*, 2007). We have used the ciliate *Tetrahymena* to show that the two centrins have distinct functions at the basal body. Mutations in either *CEN1* or *CEN2* reveal similar functions in basal body orientation and maintenance (Stemm-Wolf *et al.*, 2005; Vonderfecht *et al.*, 2011); however, our rescue experiments and other analyses demonstrate that the two genes are not redundant. This separation is deeply rooted in the evolutionary history of these genes, since the distinct functions are maintained from *Tetrahymena* to humans, as shown by the specificity of rescue of the *cen2*Δ by human *CENT3*, but not *CENT2*. In all, our data indicate that the two *Tetrahymena* centrins have similar, but not redundant, functions at basal bodies and that *Tetrahymena* basal bodies require both centrins to perform properly. The human centrin 3 can function similarly to Cen2, suggesting that the same conclusions may hold for vertebrate centrins at basal bodies.

The fact that the two centrins are distinct raises the question of what is responsible for their differences. An alignment of the two *Tetrahymena* centrins shows that the degree of sequence conservation is much lower for the NTD than the CTD. This is also true for the human centrins. This suggests that the NTDs of centrins may be responsible for the separation and distinctness of the two groups. We tested this hypothesis, utilizing chimeric proteins, and discovered that it did not hold true. Our findings from this experiment suggest a mechanism for Cen2 function (Figure 6C). The data showing that the Cen1-Cen2 chimera was able to rescue the basal body maintenance defect in the *cen2*Δ and that only the CTD of Cen2 localizes to basal bodies suggest that the CTDs of all centrins are involved in basal body localization and maintenance. However, this chimera was unable to completely rescue the orientation defect in the *cen2*Δ, suggesting that basal bodies require Cen2's distinctive NTD for proper basal body orientation. Thus it appears that both the NTD and CTD contribute to the distinct requirements for the two centrin groups.

Work with vertebrate centrins suggests that they are important for controlling the rate of centriole assembly (Yang *et al.*, 2010; Lukasiewicz *et al.*, 2011). We did not observe a change in basal body assembly rates but did see defects in basal body separation after assembly. It therefore may be possible that centrins do not function in the rate of assembly per se. Instead, defects in centriole separation may lead to defects in the rate of assembly. A centriole must first be able to properly separate from its paired centriole and undergo licensing before assembly occurs (Brownlee and Rogers, 2012). If a daughter centriole has difficulty separating from its mother in the absence of centrins, then the delay caused by this difficulty can lead to a delay in the licensing and the assembly of a new centriole. The cumulative effect would be a delay in the rate of centriole assembly. To test this notion, the rate of separation could be analyzed in vertebrate cells that contain centrin phospho-mutants

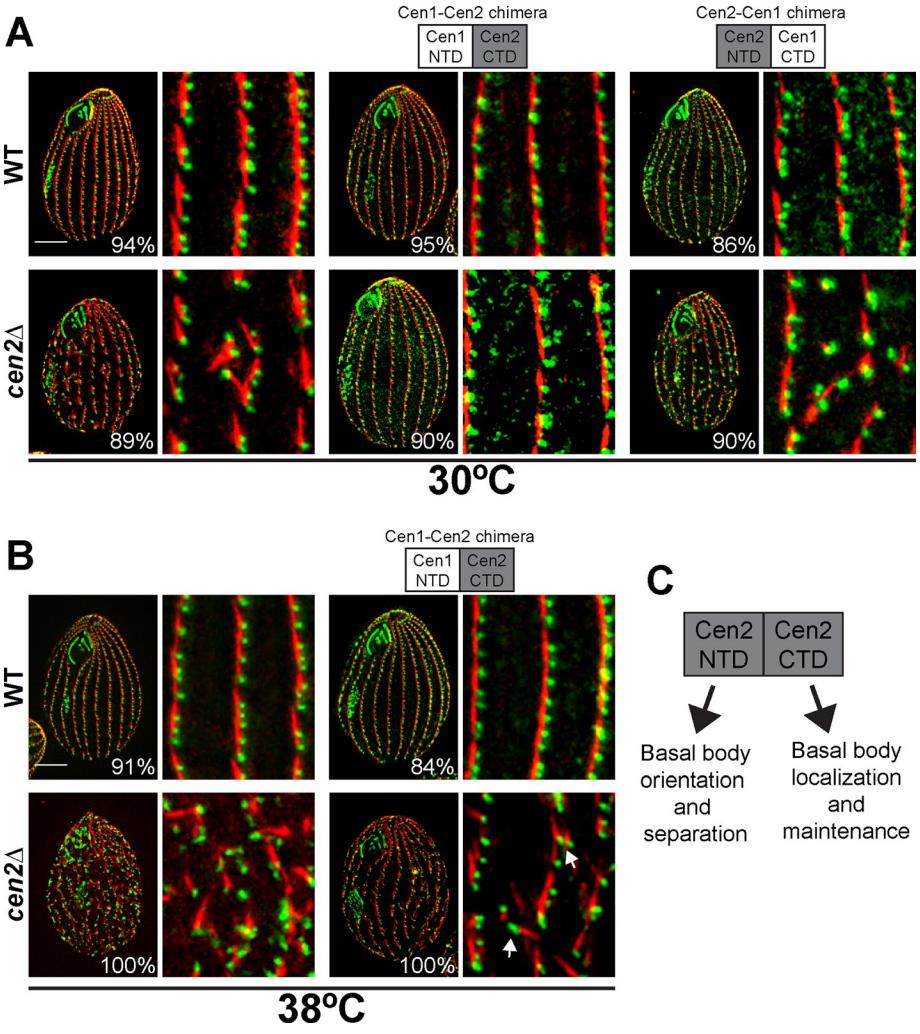


FIGURE 6: The Cen1-Cen2 chimera can rescue the loss of basal bodies in the *cen2*Δ. (A) Immunofluorescence images showing that only the Cen1-Cen2 chimera, not the Cen2-Cen1 chimera, can rescue the *cen2*Δ basal body phenotypes at 30°C. (B) Immunofluorescence images showing that the Cen1-Cen2 chimera does not rescue the basal body orientation defects (arrow) in the *cen2*Δ at 38°C. (A and B) Green, Cen1; red, KD fibers. Scale bar: 10 μm; width of insets: 10 μm. Percentages indicate the frequency of observed phenotype for 100 cells. (C) Cen2's domains have separate functions.

(Yang *et al.*, 2010; Lukasiewicz *et al.*, 2011) or in cells depleted of centrins.

The next step in fully understanding centrin's role in basal body biogenesis will require analyzing the function of its binding partners. One of the centrin binding partners that exist at basal bodies or centrioles belongs to the Sfi1 family (Kilmartin, 2003; Li *et al.*, 2006; Azimzadeh *et al.*, 2009). The Sfi1 family consists of α-helical proteins that may contain 20 or more repeats that serve as centrin binding sites (Kilmartin, 2003; Li *et al.*, 2006). The yeast Sfi1p has been shown to bind the human centrins 2 and 3 equally (Kilmartin, 2003; Martinez-Sanz *et al.*, 2006, 2010), and the human Poc5, a small protein with only three centrin binding repeats, is able to bind both human centrins, but the affinity for each is not known (Azimzadeh *et al.*, 2009). Thus the relationship of the two centrins at Sfi1 proteins is unclear. Careful studies on the interplay that occurs between the two domains of centrins and Sfi1 proteins will bring us much closer to truly understanding the functions and mechanisms of centrins and Sfi1 proteins at MTOCs.

## MATERIALS AND METHODS

### Strains and culture conditions

The wild-type *Tetrahymena thermophila* strain B2086 (*Tetrahymena* Stock Center, Cornell University, Ithaca, NY) was used in this study as the wild-type control strain. All cell lines were grown in 2% super-peptose (2% SPP) media (2% proteose peptone, 0.1% yeast extract, 0.2% glucose, and 0.003% Fe-EDTA) at 30°C or 38°C depending on the experiment. For cell-arrest experiments, cells were grown to mid–log phase in 2% SPP media, washed twice with 10 mM Tris-HCl (pH 7.4), and resuspended in 10 mM Tris-HCl (pH 7.4) at 30°C. For all experiments involving the inducible MTT promoter, induction was performed by adding $CdCl_2$ to media to 0.25 μg/ml and incubating the cells at 30°C or 38°C for 8 h before fixing or live imaging of the cells.

### DNA constructs and strain construction

Strains containing GFP-tagged full-length Cen1 or Cen2 were generated by cloning *CEN1 or CEN2* cDNA into the pENTR-D Gateway Entry Vector (Invitrogen, Carlsbad, CA). The coding sequence was then cloned into pBSmttGFPgtw (Doug Chalker, Washington University, St. Louis, MO) using the Gateway cloning system (Invitrogen). The resulting construct adds the GFP tag to the N-terminus of Cen1 or Cen2, is under control of a MTT-inducible promoter, targets for integration into the rpl29 locus, and provides cycloheximide resistance. The first 276 bases of *CEN1* were cloned into pENTR to make the Cen1 NTD, and the last 228 bases of *CEN1* were cloned into pENTR to make the Cen1 CTD. The first 270 and last 228 bases of *CEN2* were cloned into pENTR to make the Cen2 NTD and CTD, respectively. The constructs pECE-GFP-Cetn2 and pECE-GFP-Cetn3 (generous donations from H. Fisk, Ohio State University, Columbus, OH) were used to clone the human centrins into pENTR. The pENTR genes were then Gateway-cloned into pBSmttGFPgtw.

The expression of centrin genes without a tag was performed by cloning the desired gene into pBSmtt, which is under control of a MTT-inducible promoter, targets for integration into the rpl29 locus, and provides cycloheximide resistance. The Cen1-Cen2 chimera was created by PCR-stitching to create a nucleotide sequence that contained the first 276 bases of Cen1 and the last 228 bases of Cen2. Similarly, the Cen2-Cen1 chimera was created by PCR-stitching to create a nucleotide sequence with the first 270 bases of Cen2 and the last 228 bases of Cen1. The chimeras, *CEN1*, *CEN2*, and human centrin genes were all cloned into pBSmtt.

All DNA constructs were confirmed by sequencing (Macrogen USA, Rockville, MD) and were introduced into cells by biolistics and integrated into the *Tetrahymena* genome by homologous recombination (Cassidy-Hanley *et al.*, 1997). *Tetrahymena* transformants were selected by growth in SPP containing cycloheximide (15 μg/ml).

### Generation of *cen2*Δ

The *cen2*Δ was generated by creating a drug-selectable strain that has no functional *CEN2* (Hai and Gorovsky, 1997). Briefly, p4T21-CEN2del, a construct containing the *NEO2* cassette, which provides paromomycin resistance (Weide *et al*., 2007), flanked by 1.5 kb of the regions upstream and downstream of *CEN2*, was integrated at the *CEN2* locus in the micronucleus of mating wild-type *Tetrahymena* strains, B2068 or CU428 (*Tetrahymena* Stock Center) by biolistics. Strains of different mating types were made homozygous for the *NEO2* cassette at the micronucleus by mating to strains with defective micronuclei (B*VI and B*VII; *Tetrahymena* Stock Center). The resulting strains homozygous for the *NEO2* cassette at the *CEN2* locus were mated to each other to generate a new macronucleus with the *NEO2* cassette replacing *CEN2* at the *CEN2* locus. The *cen2*Δ was selected for resistance to paromomycin (100 μg/ml). Total genomic DNA was isolated by phenol:choloroform:isoamyl alcohol extraction and isopropyl alcohol precipitation (Gaertig *et al*., 1994). PCR confirmed proper integration of the *NEO2* cassette at the *CEN2* locus and deletion of *CEN2* (Figure S3A).

### Purification of recombinant Cen2

Because *Tetrahymena* stop codon usage differs from canonical stop codons, the *CEN2* gene was resynthesized for expression in *Escherichia coli* by GenScript (Piscataway, NJ). The optimized *CEN2* sequence was cloned into the *E. coli* expression vector pQE10 that adds an N-terminal 6xHis-tag to the protein. The resulting vector, pQE10-Cen2, was transformed into the *E. coli* strain M15.

The *E. coli* strain M15 containing pQE10-Cen2 was grown overnight at 37°C in Luria broth + 0.2% glucose with 50 μg/ml kanamycin and 100 μg/ml ampicillin. This culture was used to inoculate 500 ml of Luria broth, and cells were incubated at 37°C for 4 h, and then shifted to room temperature for 1 h. Expression of Cen2 was induced with 300 μM isopropyl β-D-1-thiogalactopyranoside. After 3 h, cells were pelleted, washed once with phosphate-buffered saline (PBS), and stored frozen.

Recombinant Cen2 was isolated on a nickel affinity column, as described by Stemm-Wolf *et al*. (2005). Briefly, pellets were resuspended in PBS with protease inhibitors (phenylmethylsulfonyl fluoride, leupeptin, aprotinin, and pepstatin) and lysozyme. Cells were sonicated and pelleted. The supernatant was loaded onto a Talon resin column (BD Biosciences Clontech, Palo Alto, CA), and elutions using PBS + 200 mM imidazole were collected. Fractions with Cen2 were pooled together and stored frozen in 10% glycerol. Recombinant Cen1 was purified in a similar manner, and the plasmid used to express Cen1 is described in Stemm-Wolf *et al*. (2005).

### Generation of αCen2 peptide antibody

The rabbit αCen2 peptide antibody was developed by YenZym Antibodies (San Francisco, CA). The antibody epitope consisted of a peptide containing the first 17 amino acids of the N-terminal tail of Cen2 (MNYSPKANKMKRKLKQEC). The antibody was affinity-purified using an affinity column containing recombinant Cen2 chemically ligated to AminoLink gel (Pierce Biotechnologies, Rockford, IL). The column was washed by alternating between 0.2 M glycine (pH 2.8) and 0.1 M $NaHCO_3$ (pH 8.5) + 0.5 M NaCl. The crude antibody was prepared by adding 10× TBS (Tris-buffered saline; 50 mM Tris, pH 7.5, 150 mM NaCl), 0.05% Tween, and 4 M NaCl and centrifuging the preparation. The crude preparation was incubated for 48 h in the affinity column at 4°C. Elutions using 0.2 M glycine (pH 2.8) + 0.02% NaN, were collected. Fractions containing the antibody were detected by absorbance at 280 nm and were pooled and dialyzed against PBS-azide at 4°C for 16 h.

### Fluorescence microscopy

All cell imaging, both live cell and immunofluorescence, was conducted at room temperature using an Eclipse Ti inverted microscope (Nikon, Japan) fitted with a CFI Plan-Apo VC 60×/H 1.4 numerical aperture objective (Nikon, Japan) and a CoolSNAP HQ2 charge-coupled device camera (Photometrics, Tuscon, AZ). MetaMorph Imaging software (Molecular Devices, Sunnyvale, CA) was used to collect images. The imaging software was used to analyze images by subjecting them to the nearest neighbors' deconvolution algorithm. Live-cell imaging was conducted to examine cells expressing GFP-tagged proteins. Cells were washed once with 10 mM Tris-HCl (pH 7.4), pelleted, and placed on microscope slides (VWR, Radnor, PA).

Cells examined by immunofluorescence were chemically fixed in paraformaldehyde for 10 min (Stuart and Cole, 2000). Cells were placed onto antibody slides coated with poly-L-lysine (Bellco Glass, Vineland, NJ). All primary antibodies were diluted in PBS + 1% bovine serum albumin (BSA). The affinity purified rabbit polyclonal *Tetrahymena* Centrin 2 antibody (this study) was diluted 1:100; the rabbit polyclonal *Tetrahymena* Centrin1 antibody (Stemm-Wolf *et al*., 2005) was diluted 1:1000; the mouse monoclonal 20H5 antibody raised against the *Chlamydomonas* centrin (provided by J. Salisbury, Mayo Clinic, Rochester, MN) was diluted 1:1000; the mouse monoclonal KD fiber antibody, F1-5D8, (provided by J. Frankel, University of Iowa, Iowa City, IA) was diluted 1:250; the mouse monoclonal K-like antigen antibody, 10D12 (provided by J. Frankel) was diluted 1:50; and the rabbit polyclonal *Tetrahymena* Sas6a antibody (Culver *et al*., 2009) was diluted 1:2500. Primary incubations were carried out overnight at 4°C, except for the K-like antigen antibody, which was incubated at 4°C over three nights. Following the primary incubation, cells were washed five times with PBS + 0.1% BSA. Cells were then incubated at room temperature for 1 h with secondary antibodies diluted 1:1000 in PBS + 1% BSA. The secondary antibodies used were anti-rabbit fluorescein isothiocyanate (FITC), anti-rabbit Texas Red, anti-mouse FITC, and anti-mouse Texas Red (Jackson ImmunoResearch Labs, West Grove, PA). After secondary antibody incubation, cells were washed five times with PBS + 0.1% BSA and mounted with Citifluor (Citfluor, London, United Kingdom).

### Swimming analysis

Cells were grown to mid–log phase, washed in 10 mM Tris-HCl (pH 7.4), and incubated at 30°C for 30 min. Cells were diluted to $1 \times 10^4$ cells/ml, and 5 μl of cell solution was added to standard microscope slides (VWR). Images of the cells were taken for 0.16 s at 0.02-s intervals. The distance the cells swam was measured using ImageJ (National Institutes of Health, Bethesda, MD), and the speed was calculated by dividing the distance by the time (0.168 s). Twenty cells were measured for each condition.

### Basal body new:old fluorescence ratio

Cells were grown to mid–log phase and washed in 10 mM Tris-HCl (pH 7.4). Cell arrest was carried out overnight at 30°C, and a portion of the cells was fixed. The remaining cells were released from arrest by washing them into fresh media, and after 4 h of release from arrest, cells were fixed. Fixed cells were stained with anti-Cen1 or anti-Cen2 antibodies.

The average fluorescence background signal ($F_{bkgrd}$) was measured by placing $5 \times 5$ pixel regions around the cell at areas without basal bodies and measuring the integrated fluorescence intensity

for each region with MetaMorph. Then, a basal body pair was selected, with the anterior basal body considered to be "new" and the posterior basal body "old." The integrated fluorescence intensity for each basal body ($F_i$) was measured by placing a $5 \times 5$ pixel region around the basal body, and the corrected integrated fluorescence intensity for each basal body was calculated ($F_i - F_{bkgrd}$). The distance between the two basal bodies was also measured. The basal body new:old fluorescence ratio was calculated by dividing the new basal body fluorescence by the old basal body fluorescence. For each condition, 50 basal body pairs were analyzed. For measuring all statistical differences, a Student's *t* test was performed using the Excel spreadsheet software (Microsoft, Redmond, WA).

### Quantification of basal bodies per cell

Cells progressing through the cell cycle and cells arrested in starvation media (10 mM Tris-HCl, pH 7.4) were analyzed. Cells were stained with the anti-Cen1 antibody to label basal bodies. For cells progressing through the cell cycle, cells in oral primordium stages 1–2 were analyzed to ensure that the quantification was done at a consistent cell cycle stage (Bakowska *et al.*, 1982). The Count Particles function of the program ImageJ was used to count the basal bodies across the entire cell surface area. A total of 25 cells were analyzed for each condition.

### Quantification of basal bodies per micrometer

Cells progressing through the cell cycle at oral primordium stages 1–2 were stained with the anti-Cen1 antibody to label basal bodies. The number of basal bodies along a 10-µm length of a ciliary row was counted and subsequently divided by 10 µm to get the number of basal bodies per 1 µm. The mean cell length was measured to ensure that changes in basal body frequency were not a result of changes in cell length. A total of five measurements in 10 cells was analyzed to get 50 measurements for each condition.

### Basal body angle

Cells were stained with the anti-Cen1 and KD fiber antibodies to label basal bodies and their orientation in the cell. Basal body angle was calculated by measuring the angle of two basal bodies from the anterior–posterior axis of the cell using the ImageJ program. A total of 100 measurements were made for each condition. Circular plots were constructed using the Oriana program (Kovach Computing Services, Pentraeth, Wales, UK).

### EM

*Tetrahymena* cells were prepared for ultrastructural analysis and immunolocalization of Cen2 by high-pressure freezing followed by freeze substitution (Giddings *et al.*, 2010; Meehl *et al.*, 2010). Briefly, cells were centrifuged into a cryoprotectant solution consisting of 15% dextran (9–11 kDa; Sigma-Aldrich) and 5% BSA in 10 mM Tris-HCl (pH 7.4). The resulting loose pellet was high-pressure frozen in a Bal-Tec HPM-010 (Leica Microsystems, Wetzlar, Germany), then freeze-substituted in 0.25% glutaraldehyde and 0.1% uranyl acetate in acetone and embedded in Lowicryl HM20.

Nickel grids containing ribbons of 15–20 serial 60-nm–thick sections were prepared for immuno-EM by incubating them in blocking solution (1% nonfat dry milk dissolved in PBS-Tween 20 [0.1%]) and then in blocking solution containing the rabbit polyclonal Cen2 antibody (diluted 1:5) or the rabbit polyclonal anti-GFP antibody (diluted 1:200; provided by C. Pearson, University of Colorado–Denver, Denver, CO). The 10- or 15-nm gold-conjugated anti-rabbit secondary antibody was applied to the grids (Ted Pella, Redding, CA). Grids were poststained with 2% uranyl acetate and lead citrate. Samples were imaged using a Philips CM 10 (FEI, Hillsboro, OR) equipped with a Gatan BioScan digital camera (Gatan, Pleasanton, CA) or a Philips CM 100 transmission electron microscope equipped with an AMT V600 digital camera (Advanced Microscopy Techniques, Danvers, MA). Six basal body domains were identified by morphological criteria (Kilburn *et al.*, 2007). Gold particles on each serial cross-section through the basal bodies were counted and assigned to these domains.

### PCR/RT-PCR

Genomic DNA was isolated from *Tetrahymena* cells by phenol:chloroform:isoamyl alcohol extraction, which was followed by precipitation with isopropanol, as described previously. PCR with Phusion polymerase (New England Biolabs, Ipswich, MA) was performed with 0.25 µg of genomic DNA. PCR was carried out according to the manufacturer's instructions. RT-PCR was performed using the SuperScript III One-Step RT-PCR System with Platinum *Taq* High Fidelity kit (Invitrogen).

Samples were run in a 1% Tris-acetate-EDTA agarose gel. The gel was stained with ethidium bromide and viewed through a FOTO/Analyst Investigator Eclipse workstation (FOTODYNE, Hartland, WI).

### Western blot analysis

Whole-cell extracts were prepared by lysing ~30,000 cells in sample buffer (20% glycerol, 2% SDS, 125 mM Tris, pH 6.8, 5% β-mercaptoethanol) and heating to 80°C for 4 min. Approximately 2250 cell equivalents were loaded in lanes in 4–20% Precise Protein precast gels (Pierce, Rockford, IL). For recombinant proteins, ~0.5 mg/ml was added to each lane of the gel. Proteins were transferred to Immobilon membranes (Millipore, Billerica, MA) using a transfer apparatus (Bio-Rad Labs, Hercules, CA). Membranes were blotted in TBS containing 0.05% Tween and 2% BSA. Primary antibodies (rabbit polyclonal anti-Cen1 antibody, rabbit polyclonal Cen2 antibody, mouse polyclonal anti–6x histidine ascites [Babco International, Inc., Tucson, AZ], and mouse monoclonal B-5-1-2 anti–α-tubulin antibody [Sigma-Aldrich, St. Louis, MO]) were diluted 1:1000 into TBS containing 0.05% Tween and 2% BSA. Primary antibody was incubated overnight at 4°C, and membranes were washed three times with TBS containing 0.05% Tween. Secondary antibodies (anti–rabbit IR800 and anti–mouse IR680 [LI-COR Biosciences, Lincoln, NE]) were diluted 1:10,000 into TBS containing 0.05% Tween and 2% BSA. Secondary antibody incubations were performed at room temperature for 1 h and were followed by three washes with TBS containing 0.05% Tween. Blots were visualized on a LI-COR Odyssey scanner.

## ACKNOWLEDGMENTS

We thank Alex Stemm-Wolf, Chad Pearson, and Anne Aubusson-Fleury for advice and helpful discussions; Joe Frankel and Jeffrey Salisbury for antibodies; Harold Fisk for the human centrin plasmids; and Alex Stemm-Wolf and Melissa Hendershott for plasmids. This work was supported by National Institutes of Health grants GM074746 (to M.W.) and F31 GM095071 (to T.V.).

## REFERENCES

Allen RD (1969). The morphogenesis of basal bodies and accessory structures of the cortex of the ciliated protozoan *Tetrahymena pyriformis*. J Cell Biol 40, 716–733.

Andersen JR, Wilkinson CJ, Mayor T, Mortensen P, Nigg EA, Mann M (2003). Proteomic characterization of the human centrosome by protein correlation profiling. Nature 426, 570–574.

Aubusson-Fleury A, Lemullois M, de Loubresse NG, Laligné C, Cohen J, Rosnet O, Jerka-Dziadosz M, Beisson J, Koll F (2012). FOR20, a

conserved centrosomal protein, is required for assembly of the transition zone and basal body docking at the cell surface. J Cell Sci 125, 4395–4404.
Azimzadeh J, Hergert P, Delouvée A, Euteneuer U, Formstecher E, Khodjakov A, Bornens M (2009). hPOC5 is a centrin-binding protein required for assembly of full-length centrioles. J Cell Biol 185, 101–114.
Badano JL, Mitsuma N, Beales PL, Katsanis N (2006). The ciliopathies: an emerging class of human genetic disorders. Annu Rev Genomics Hum Genet 7, 125–148.
Bakowska J, Frankel J, Nelsen EM (1982). Regulation of the pattern of basal bodies within the oral apparatus of *Tetrahymena thermophila*. J Embryol Exp Morph 69, 83–105.
Baum P, Furlong C, Byers B (1986). Yeast gene required for spindle pole body duplication: homology of its product with $Ca^{2+}$-binding proteins. Proc Natl Acad Sci USA 83, 5512–5516.
Bornens M, Azimzadeh J (2007). Origin and evolution of the centrosome. Adv Exp Med Biol 607, 119–129.
Brownlee C, Rogers G (2012). Show me your license, please: deregulation of centriole duplication mechanisms that promote amplification. Cell Mol Life Sci, DOI: 10.1007/s00018-012-1102-6.
Byers B (1981). Multiple roles of the spindle pole bodies in the life cycle of *Saccharomyces cerevisiae*. Molecular Genetics in Yeast: Proceedings of the Alfred Benzon Symposium 16, ed. DV Wettstein, Copenhagen, Denmark: Munksgaard, 119–131.
Carvalho-Santos Z, Azimzadeh J, Pereira-Leal JB, Bettencourt-Dias M (2011). Tracing the origins of centrioles, cilia, and flagella. J Cell Biol 194, 165–175.
Cassidy-Hanley D, Bowen J, Lee JH, Cole E, VerPlank LA, Gaertig J, Gorovsky MA, Bruns PJ (1997). Germline and somatic transformation of mating *Tetrahymena thermophila* by particle bombardment. Genetics 146, 135–147.
Culver BP, Meehl JB, Giddings TH, Jr., Winey M (2009). The two SAS-6 homologs in *Tetrahymena thermophila* have distinct functions in basal body assembly. Mol Biol Cell 20, 1865–1877.
Dantas TJ, Wang Y, Lalor P, Dockery P, Morrison CG (2011). Defective nucleotide excision repair with normal centrosome structures and functions in the absence of all vertebrate centrins. J Cell Biol 193, 307–318.
Delaval B, Covassin L, Lawson ND, Doxsey S (2011). Centrin depletion causes cyst formation and other ciliopathy-related phenotypes in zebrafish. Cell Cycle 10, 3964–3972.
Frankel J (2000). Cell biology of *Tetrahymena thermophila*. Methods Cell Biol 62, 27–125.
Gaertig J, Gu L, Hai B, Gorovsky MA (1994). High frequency vector-mediated transformation and gene replacement in *Tetrahymena*. Nucleic Acids Res 22, 5391–5398.
Geimer S, Melkonian M (2005). Centrin scaffold in *Chlamydomonas reinhardtii* revealed by immunoelectron microscopy. Eukaryotic Cell 4, 1253–1263.
Giddings TH, Jr., Meehl JB, Pearson CG, Winey M (2010). Electron tomography and immuno-labeling of *Tetrahymena thermophila* basal bodies. Methods Cell Biol 96, 117–141.
Graser S, Stierhof Y-D, Lavoie SB, Gassner OS, Lamla S, Le Clech M, Nigg EA (2007). Cep164, a novel centriole appendage protein required for primary cilium formation. J Cell Biol 179, 321–330.
Hai B, Gorovsky MA (1997). Germ-line knockout heterokaryons of an essential α-tubulin gene enable high-frequency gene replacement and a test of gene transfer from somatic to germ-line nuclei in *Tetrahymena thermophila*. Proc Natl Acad Sci USA 94, 1310–1315.
Hartwell L, Mortimer R, Culotti J, Culotti M (1973). Genetic control of the cell division cycle in yeast: V. genetic analysis of cdc mutants. Genetics 74, 267–286.
Hodges ME, Scheumann N, Wickstead B, Langdale JA, Gull K (2010). Reconstructing the evolutionary history of the centriole from protein components. J Cell Sci 123, 1407–1413.
Hu H, Chazin WJ (2003). Unique features in the C-terminal domain provide caltractin with target specificity. J Mol Biol 330, 473–484.
Huang B, Mengersen A, Lee VD (1988). Molecular cloning of cDNA for caltractin, a basal body-associated $Ca^{2+}$-binding protein: homology in its protein sequence with calmodulin and the yeast *CDC31* gene product. J Cell Biol 107, 133–140.
Jaspersen SL, Winey M (2004). The budding yeast spindle pole body: structure, duplication, and function. Annu Rev Cell Dev Biol 20, 1–28.
Kaczanowski A (1978). Gradients of proliferation of ciliary basal bodies and the determination of the position of the oral primordium in *Tetrahymena*. J Exp Zool 204, 417–430.
Keller LC, Romijn EP, Zamora I, Yates JR, Marshall WF (2005). Proteomic analysis of isolated *Chlamydomonas* centrioles reveals orthologs of ciliary-disease genes. Curr Biol 15, 1090–1098.
Kilburn CL, Pearson CG, Romijn EP, Meehl JB, Giddings TH, Jr., Culver BP, Yates JR, III, Winey M (2007). New *Tetrahymena* basal body protein components identify basal body domain structure. J Cell Biol 178, 905–912.
Kilmartin JV (2003). Sfi1p has conserved centrin-binding sites and an essential function in budding yeast spindle pole body duplication. J Cell Biol 162, 1211–1221.
Kleylein-Sohn J, Westendorf J, Le Clech M, Habedanck R, Stierhof Y-D, Nigg EA (2007). Plk4-induced centriole biogenesis in human cells. Dev Cell 13, 190–202.
Koblenz B, Schoppmeier J, Grunow A, Lechtreck KF (2003). Centrin deficiency in *Chlamydomonas* causes defects in basal body replication, segregation and maturation. J Cell Sci 116, 2635–2646.
Laoukili J, Perret E, Middendorp S, Houcine O, Guennou C, Marano F, Bornens M, Tournier F (2000). Differential expression and cellular distribution of centrin isoforms during human ciliated cell differentiation in vitro. J Cell Sci 113, 1355–1364.
LeDizet M, Beck JC, Finkbeiner WE (1998). Differential regulation of centrin genes during ciliogenesis in human tracheal epithelial cells. Am J Physiol Lung Cell Mol Physiol 275, L1145–L1156.
Li S, Sandercock AM, Conduit P, Robinson CV, Williams RL, Kilmartin JV (2006). Structural role of Sfi1p-centrin filaments in budding yeast spindle pole body duplication. J. Cell Biol. 173, 867–877.
Liu Q, Tan G, Levenkova N, Li T, Pugh EN, Rux JJ, Speicher DW, Pierce EA (2007). The proteome of the mouse photoreceptor sensory cilium complex. Mol Cell Proteomics 6, 1299–1317.
Lukasiewicz KB, Greenwood TM, Negron VC, Bruzek AK, Salisbury JL, Lingle WL (2011). Control of centrin stability by Aurora A. PLoS One 6, e21291.
Marshall WF, Kintner C (2008). Cilia orientation and the fluid mechanics of development. Curr Opin Cell Biol 20, 48–52.
Marshall WF, Nonaka S (2006). Cilia: tuning in to the cell's antenna. Curr Biol 16, R604–R614.
Martinez-Sanz J, Kateb F, Assairi L, Blouquit Y, Bodenhausen G, Abergel D, Mouawad L, Craescu CT (2010). Structure, dynamics and thermodynamics of the human centrin 2/hSfi1 complex. J Mol Biol 395, 191–204.
Martinez-Sanz J, Yang A, Blouquit Y, Duchambon P, Assairi L, Craescu CT (2006). Binding of human centrin 2 to the centrosomal protein hSfi1. FEBS J 273, 4504–4515.
Matei E, Miron S, Blouquit Y, Duchambon P, Durussel I, Cox JA, Craescu CT (2003). C-terminal half of human centrin 2 behaves like a regulatory EF-hand domain. Biochem 42, 1439–1450.
Meehl JB, Giddings TH, Winey M (2010). Gavin RH (2010). High pressure freezing, electron microscopy, and immuno-electron microscopy of Tetrahymena thermophila basal bodies. In: Cytoskeleton Methods and Protocols 586, New York: Humana Press, 227–241.
Miao W, Xiong J, Bowen J, Wang W, Liu Y, Braguinets O, Grigull J, Pearlman RE, Orias E, Gorovsky MA (2009). Microarray analyses of gene expression during the *Tetrahymena thermophila* life cycle. PLoS One 4, e4429.
Middendorp S, Kuntziger T, Abraham Y, Holmes S, Bordes N, Paintrand M, Paoletti A, Bornens M (2000). A role for centrin 3 in centrosome reproduction. J Cell Biol 148, 405–415.
Middendorp S, Paoletti A, Schiebel E, Bornens M (1997). Identification of a new mammalian centrin gene, more closely related to *Saccharomyces cerevisiae* CDC31 gene. Proc Natl Acad Sci USA 94, 9141–9146.
Paoletti A, Moudjou M, Paintrand M, Salisbury JL, Bornens M (1996). Most of centrin in animal cells is not centrosome-associated and centrosomal centrin is confined to the distal lumen of centrioles. J Cell Sci 109, 3089–3102.
Pearson CG, Winey M (2009). Basal body assembly in ciliates: the power of numbers. Traffic 10, 461–471.
Pearson CG, Giddings TH, Jr., Winey M (2009). Basal body components exhibit differential protein dynamics during nascent basal body assembly. Mol Biol Cell 20, 904–914.
Ruiz F, Garreau de Loubresse N, Klotz C, Beisson J, Koll F (2005). Centrin deficiency in *Paramecium* affects the geometry of basal-body duplication. Curr Biol 15, 2097–2106.
Salisbury JL, Baron A, Surek B, Melkonian M (1984). Striated flagellar roots: isolation and partial characterization of a calcium-modulated contractile organelle. J Cell Biol 99, 962–970.

Salisbury J, Suino K, Busby R, Springett M (2002). Centrin-2 is required for centriole duplication in mammalian cells. Curr Biol 12, 1287–1292.

Sanders M, Salisbury J (1994). Centrin plays an essential role in microtubule severing during flagellar excision in *Chlamydomonas reinhardtii*. J Cell Biol 124, 795–805.

Selvapandiyan A, Kumar P, Salisbury JL, Wang CC, Nakhasi HL (2012). Role of centrins 2 and 3 in organelle segregation and cytokinesis in *Trypanosoma brucei*. PLoS One 7, e45288.

Shang Y, Li B, Gorovsky MA (2002). *Tetrahymena thermophila* contains a conventional γ-tubulin that is differentially required for the maintenance of different microtubule-organizing centers. J Cell Biol 158, 1195–1206.

Spang A, Courtney I, Fackler U, Matzner M, Schiebel E (1993). The calcium-binding protein division cycle 31 of *Saccharomyces cerevisiae* is a component of the half bridge of the spindle pole body. J Cell Biol. 123, 405–416.

Stemm-Wolf AJ, Morgan G, Giddings TH, Jr., White EA, Marchione R, McDonald HB, Winey M (2005). Basal body duplication and maintenance require one member of the *Tetrahymena thermophila* centrin gene family. Mol Biol Cell 16, 3606–3619.

Strnad P, Leidel S, Vinogradova T, Euteneuer U, Khodjakov A, Gönczy P (2007). Regulated HsSAS-6 levels ensure formation of a single procentriole per centriole during the centrosome duplication cycle. Dev Cell 13, 203–213.

Stuart KR, Cole ES (2000). Nuclear and cytoskeletal fluorescence microscopy techniques. Methods Cell Biol 62, 291–311.

Thompson JR, Ryan ZC, Salisbury JL, Kumar R (2006). The structure of the human centrin 2-xeroderma pigmentosum group C protein complex. J Biol Chem 281, 18746–18752.

Veeraraghavan S, Fagan PA, Hu H, Lee V, Harper JF, Huang B, Chazin WJ (2002). Structural independence of the two EF-hand domains of caltractin. J Biol Chem 277, 28564–28571.

Vonderfecht T, Stemm-Wolf AJ, Hendershott M, Giddings TH, Meehl JB, Winey M (2011). The two domains of centrin have distinct basal body functions in *Tetrahymena*. Mol Biol Cell 22, 2221–2234.

Weide T, Bockau U, Rave A, Herrmann L, Hartmann M (2007). A recombinase system facilitates cloning of expression cassettes in the ciliate *Tetrahymena thermophila*. BMC Microbiol 7, 12.

Williams NE, Honts JE, Kaczanowska J (1990). The formation of basal body domains in the membrane skeleton of *Tetrahymena*. Development 109, 935–942.

Wolfe J (1970). Structural analysis of basal bodies of the isolated oral apparatus of *Tetrahymena pyriformis*. J Cell Sci 6, 679–700.

Wolfrum U, Salisbury JL (1998). Expression of centrin isoforms in the mammalian retina. Exp Cell Res 242, 10–17.

Yang A, Miron S, Duchambon P, Assairi L, Blouquit Y, Craescu CT (2005). The N-terminal domain of human centrin 2 has a closed structure, binds calcium with a very low affinity, and plays a role in the protein self-assembly. Biochem 45, 880–889.

Yang C-H, Kasbek C, Majumder S, Yusof AM, Fisk HA (2010). Mps1 phosphorylation sites regulate the function of centrin 2 in centriole assembly. Mol Biol Cell 21, 4361–4372.